Healthcraft Frontiers
https://www.acadlore.com/journals/HF

Evaluating the Efficacy of Tuberculosis Management Strategies in Nigeria: A Mathematical Modelling Approach

Jafar Anafi[1*], Sharhabil Tasiu[2]

[1] Department of Public Policy, Helpman Development Institute, 900110 Abuja, Nigeria
[2] Department of Public Health, Helpman Development Institute, 900110 Abuja, Nigeria

[*] Correspondence: Jafar Anafi (janafi@helpmaninstitute.org)

Received: 12-20-2023 **Revised:** 02-15-2024 **Accepted:** 02-24-2024

Citation: Anafi, J. & Tasiu, S. (2023). Evaluating the efficacy of tuberculosis management strategies in Nigeria: A mathematical modelling approach. *Healthcraft Front.*, *2*(1), 46-58. https://doi.org/10.56578/hf020105.

Abstract: Tuberculosis (TB), an airborne disease caused by Mycobacterium, poses a significant global health challenge due to its rapid transmission through air and interaction with infected individuals. This study presents a comprehensive dynamic model to assess the impact of TB treatment and vaccination strategies in Nigeria, focusing on the comparative analysis of untreated and treated populations, as well as evaluating mortality and recovery outcomes. Through simulations conducted using the Berkeley Madonna Software, it was observed that the populations of latent and susceptible individuals exhibit a near-equivalence, yet the cohort undergoing treatment markedly surpasses other groups. Interestingly, the infected demographic aligns closely with the average values across all compartments. An alarming trend was noted in chronic patients, whose numbers initially increase, followed by a decline over a six-year period, and then a subsequent rise, while the count of treated individuals demonstrates a continuous decrease. The study further reveals a pressing need for treatment among vaccinated individuals, highlighting a nuanced interplay between vaccination and therapeutic interventions. By employing stability and sensitivity analyses, this research underscores the critical importance of treatment in managing TB infection, advocating for enhanced strategies to mitigate the spread of this infectious disease. The findings contribute valuable insights into the dynamics of TB infection and the pivotal role of treatment, underscoring the necessity for integrated approaches in addressing the TB epidemic, particularly in regions burdened by high infection rates.

Keywords: Tuberculosis infection; Stability analysis; Sensitivity analysis; Treatment impact; Vaccination strategy

1. Introduction

TB is a global illness that mainly affects the lungs and is caused by Mycobacterium, which can be spread when an individual with the illness coughs, sneezes, or sings, passing through the air to susceptible individuals. TB is one of the most contagious diseases, claiming more lives every day (World Health Organization, 2019). In the exploration of TB management strategies, Sulayman & Abdullah (2022) identified a significant distinction between the approaches to health education and the lack thereof, which divided infectious individuals into two classes: infected individuals treated at home versus those treated in hospital settings (Huo & Zou, 2016). In every population, at least one-third has a TB disease, which yields millions of deaths and new cases annually (Castillo-Chavez & Song, 2004; Sudre et al., 1992; Ullah et al., 2019). In order to identify ways to control diseases in the population, several studies have been conducted in mathematical modelling (Atangana & Doungmo Goufo, 2014; Goufo et al., 2016; Goufo et al., 2017; Leon et al., 2017; Ndondo et al., 2016; Tchepmo Djomegni et al., 2018), which is developed and applied to the spread of diseases in order to understand the epidemiological transition phenomenon (Kasereka et al., 2014; Kasereka, et al., 2018) at different locations.

Every country has different scenarios, but there are major surprises when it comes to Nigerians in terms of diseases. Some Nigerians don't go to the hospital before they get cured of their illness, because maybe they have a strong immune system, lack money or don't believe in hospital treatment. In fact, some people go to the clinic/chemist that they can afford. Chemists provide a healthcare centre where individuals get treated at a low price, but the healthcare officer at the place is not professional. Some formal doctors used to call them quack

doctors (which means unprofessional) because they did not want formal education. These people are healthcare providers with professional training and are acquainted with their boss. Some individuals go to either a secondary or tertiary hospital for treatment. This study focuses on people with TB who try medication or treatment, as well as those who do not take medication or treatment or go to the hospital. How can they get cured? Some research (Saito & Nagasaki, 2008) shows that individuals with high-level melanin hormone can get cured because the hormone fights the virus to some extent. The model proposed in this study presents the transmission dynamics of TB among individuals, examining scenarios both in the presence and absence of treatment interventions. The motive behind this is because TB is among the most communicable diseases in the world. The model reveals that some individuals recover without treatment at each stage, while others become chronically infected, rendering them incurable. They have to return home for treatment, and some people got vaccinated to avoid being infected. After the treatment, all the individuals move to the susceptible group so that the process can start again and again. This work designed a model for TB, incorporating both treated and untreated scenarios. Nigeria was used as a pilot. The model was analysed using a compartmental modelling approach to study the transmission dynamics of TB at different stages of infection.

2. Model Description

Figure 1 presents a four-compartment model. In the model, the S population is considered as susceptible people who have not contacted TB with a birth rate of $\mu(1\text{-}p)N$, where $(1\text{-}p)$ is the unvaccinated individual rate with a death rate of μ. The S group can contract TB with a rate of $\beta F_{SL}\frac{1}{N}$ to the latent (L) stage, in which the L individual can return to S with a rate of γ without going to the hospital or taking drugs. It can be noted that the L individual can become infectious (I) with the contact rate of F_{LI}, and the transmission rate of δ can be revised to α with a death rate of μ. The L individual can also be treated (T) without becoming I if he can be detected early with a rate of p. An I individual can also directly become T at a rate of r_2. The T individual can also become I at a contact rate of ϵ and a transmission rate of F_{TI} if he is in the chronic stage. In this case, he cannot be T because the drugs do not work for him any more, or the disease is not cured. During hospitalization or treatment, the individual can also become L (not able to get I due to the drugs taken in the hospital), with a death rate of μ. Before leaving the hospital, it is assumed that all the T individuals are vaccinated at the rate of μP. Then all the survival treatment moves to S at a rate of q. After the vaccine has expired, the individual can be I again.

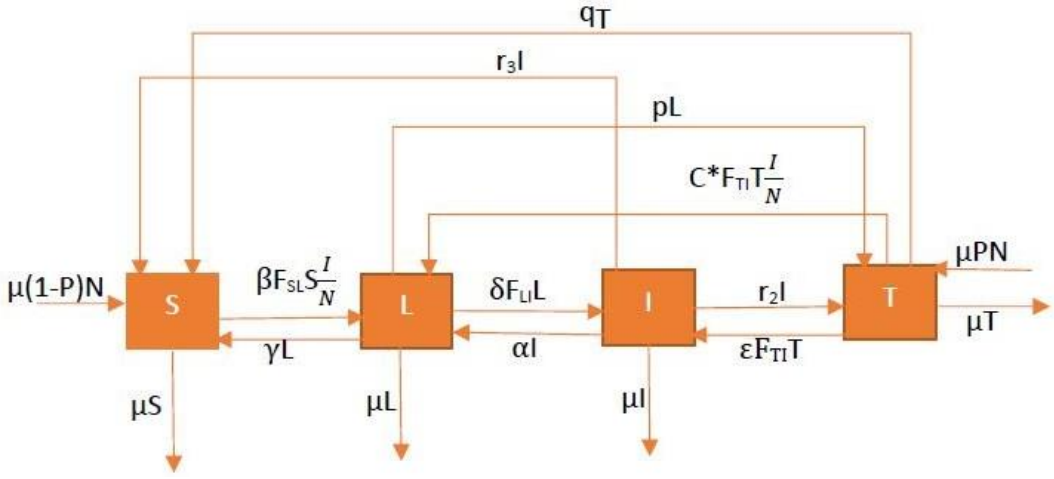

Figure 1. The four-compartment model

2.1 Mathematical Model

The number of S individuals increases and decreases as a result of natural death and latent infection at rates of $\mu(1\text{-}p)$, r_3, q, γ with respect to the total population (N), I, T and μ, β, respectively. Therefore, the change rates of susceptible populations are given as follows:

$$\frac{dS}{dt} = \mu(1-p)N + r_3 I + qT + \gamma L - \beta F_{SL} S\frac{I}{N} - \mu S \tag{1}$$

The S populations are exposed and get I at the rate of β with a transmission rate of F_{SL} and decreased as a result of death due to L at a rate of μ; others also contribute to the population from T and I.

$$\frac{dL}{dt} = \beta F_{SL} S \frac{I}{N} + C^* F_{TL} T \frac{I}{N} + \alpha I - \delta F_{LI} L - \gamma L - pL - \mu L \tag{2}$$

Similarly, the I population is cured after being T at a rate of r_2 and dead at a rate of μ.

$$\frac{dI}{dt} = \delta F_{LI} L + \epsilon F_{TI} T - \alpha I - r_3 I - r_2 I - \mu I \tag{3}$$

Finally, the T population is generated via the recovery of I individuals in the L stage and vaccinated individuals with a rate of μ and a vaccination rate of P. It can be seen from the equation that some individuals also return to both I (due to no response to treatment) and L (due to being partially cured to the extent that he/she cannot infect the population).

$$\frac{dT}{dt} = pL + r_2 I + \mu PN - qT - C^* F_{TL} T \frac{I}{N} - \epsilon F_{TI} T - \mu T \tag{4}$$

Therefore, based on the above descriptions and assumptions, the TB model, incorporating both treated and untreated scenarios, culminates in the derivation of a set of non-linear differential equations.

$$\mathbf{F}(t) = \begin{cases} \frac{dS}{dt} = \mu(1-p)N + r_3 I + qT + \gamma L - \beta F_{SL} S \frac{I}{N} - \mu S \\ \frac{dL}{dt} = \beta F_{SL} S \frac{I}{N} + C^* F_{TL} T \frac{I}{N} + \alpha I - \delta F_{LI} L - \gamma L - pL - \mu L \\ \frac{dI}{dt} = \delta F_{LI} L + \epsilon F_{TI} T - \alpha I - r_3 I - r_2 I - \mu I \\ \frac{dT}{dt} = pL + r_2 I + \mu PN - qT - C^* F_{TL} T \frac{I}{N} - \epsilon F_{TI} T - \mu T \end{cases} \tag{5}$$

2.2 Equilibrium State

Equilibrium changes in $\frac{dS}{dt} = \frac{dL}{dt} = \frac{dI}{dt} = \frac{dT}{dt} = 0$ yields:

$$0 = \mu(1-p)N + r_3 I + qT + \gamma L - \beta F_{SL} S \frac{I}{N} - \mu S \tag{6}$$

$$0 = \beta F_{SL} S \frac{I}{N} + C^* F_{TL} T \frac{I}{N} + \alpha I - \delta F_{LI} L - \gamma L - pL - \mu L \tag{7}$$

$$0 = \delta F_{LI} L + \epsilon F_{TI} T - \alpha I - r_3 I - r_2 I - \mu I \tag{8}$$

$$0 = pL + r_2 I + \mu PN - qT - C^* F_{TL} T \frac{I}{N} - \epsilon F_{TI} T - \mu T \tag{9}$$

At the initial stage, it is assumed that nothing is recorded, i.e., $L = 0$, $I = 0$, $T = 0$, and then it yields:

$$\mu S = \mu(1-p)N + r_3 * 0 + q * 0 + \gamma * 0 - \beta S F_{SL} \frac{0}{N}$$

$$S = (1-P)N$$

The TB-free equilibrium is $E = (S, L, I, T) = ((1 - P)N, 0, 0, 0)$.

2.3 Stability of the Disease-Free Equilibrium

$$D\mathbf{F}(t) = \begin{bmatrix} \frac{\partial S'}{\partial S} & \frac{\partial S'}{\partial L'} & \frac{\partial S'}{\partial I} & \frac{\partial S'}{\partial T'} \\ \frac{\partial L'}{\partial S} & \frac{\partial L'}{\partial L'} & \frac{\partial L'}{\partial I} & \frac{\partial L'}{\partial T'} \\ \frac{\partial I'}{\partial S} & \frac{\partial I'}{\partial L} & \frac{\partial I'}{\partial I} & \frac{\partial I'}{\partial T} \\ \frac{\partial T'}{\partial S} & \frac{\partial T'}{\partial L} & \frac{\partial T'}{\partial I} & \frac{\partial T'}{\partial T} \end{bmatrix} \tag{10}$$

$$D\mathbf{F}(t)=\begin{bmatrix} -\beta F_{SL}\dfrac{I}{N}-\mu & \gamma & r_3+\beta SF_{SL}\dfrac{1}{N} & q \\ \beta F_{SL}\dfrac{I}{N} & -\delta F_{LI}-\gamma-p-\mu & \beta SF_{SL}\dfrac{1}{N}+C^*F_{TL}T\dfrac{1}{N}+\alpha & C^*F_{TL}\dfrac{I}{N} \\ 0 & \delta F_{LI} & -\alpha-r_3-r_2-\mu & \epsilon F_{TI} \\ 0 & p & r_2-C^*F_{TL}T\dfrac{1}{N} & -q-C^*F_{TL}\dfrac{I}{N}-\epsilon F_{TI}-\mu \end{bmatrix} \tag{11}$$

The eigenvalue is $A-\lambda I=0$, which means that the function $\mathrm{F}(t)=0$ and $A=\mathrm{DF}(t)$.

$$A-\lambda I=\begin{bmatrix} -\beta F_{SL}\dfrac{I}{N}-\mu-\lambda & \gamma & r_3+\beta SF_{SL}\dfrac{1}{N} & q \\ \beta F_{SL}\dfrac{I}{N} & -\delta F_{LI}-\gamma-p-\mu-\lambda & \beta SF_{SL}\dfrac{1}{N}+C^*F_{TL}T\dfrac{1}{N}+\alpha & C^*F_{TL}\dfrac{I}{N} \\ 0 & \delta F_{LI} & -\alpha-r_3-r_2-\mu-\lambda & \epsilon F_{TI} \\ 0 & p & r_2-C^*F_{TL}T\dfrac{1}{N} & -q-C^*F_{TL}\dfrac{I}{N}-\epsilon F_{TI}-\mu-\lambda \end{bmatrix}=0$$

The characteristic equation of the function $A-\lambda I=0$ is as follows:

$$-\beta F_{SL}\frac{I}{N}-\mu-\lambda\begin{bmatrix} -\delta F_{LI}-\gamma-p-\mu-\lambda & \beta SF_{SL}\dfrac{1}{N}+C^*F_{TL}T\dfrac{1}{N}+\alpha & C^*F_{TL}\dfrac{I}{N} \\ \delta F_{LI} & -\alpha-r_3-r_2-\mu-\lambda & \epsilon F_{TI} \\ p & r_2-CF_{TL}T\dfrac{1}{N} & -q-C^*F_{TL}\dfrac{I}{N}-\epsilon F_{TI}-\mu-\lambda \end{bmatrix}$$

$$-\gamma\begin{bmatrix} \beta F_{SL}\dfrac{I}{N} & \beta SF_{SL}\dfrac{1}{N}+C^*F_{TL}T\dfrac{1}{N}+\alpha & C^*F_{TL}\dfrac{I}{N} \\ 0 & -\alpha-r_3-r_2-\mu-\lambda & \epsilon F_{TI} \\ 0 & r_2-C^*F_{TL}T\dfrac{1}{N} & -q-C^*F_{TL}\dfrac{I}{N}-\epsilon F_{TI}-\mu-\lambda \end{bmatrix}$$

$$r_3+\beta SF_{SL}\frac{1}{N}\begin{bmatrix} \beta F_{SL}\dfrac{I}{N} & -\delta F_{LI}-\gamma-p-\mu-\lambda & CF_{TL}\dfrac{I}{N} \\ 0 & \delta F_{LI} & \epsilon F_{TI} \\ 0 & p & -q-C^*F_{TL}\dfrac{I}{N}-\epsilon F_{TI}-\mu-\lambda \end{bmatrix}+$$

$$-q\begin{bmatrix} \beta F_{SL}\dfrac{I}{N} & -\delta F_{LI}-\gamma-p-\mu-\lambda & \beta SF_{SL}\dfrac{1}{N}+C^*F_{TL}T\dfrac{1}{N}+\alpha \\ 0 & \delta F_{LI} & -\alpha-r_3-r_2-\mu-\lambda \\ 0 & p & r_2-C^*F_{TL}T\dfrac{1}{N} \end{bmatrix}=0$$

When the TB-free is substituted with $A-\lambda I$, it yields:

$$A-\lambda I=\begin{bmatrix} -\mu-\lambda & \gamma & r_3 & q \\ 0 & -\delta F_{LI}-\gamma-p-\mu-\lambda & \alpha & 0 \\ 0 & \delta F_{LI} & -\alpha-r_3-r_2-\mu-\lambda & \epsilon F_{TI} \\ 0 & p & r_2 & -q-\epsilon F_{TI}-\mu-\lambda \end{bmatrix}=0$$

The characteristic equation of the function $A-\lambda I=0$ is as follows:

$$-\mu-\lambda\begin{bmatrix} -\delta F_{LI}-\gamma-p-\mu-\lambda & \alpha & 0 \\ \delta F_{LI} & -\alpha-r_3-r_2-\mu-\lambda & \epsilon F_{TI} \\ p & r_2 & -q-\epsilon F_{TI}-\mu-\lambda \end{bmatrix}-\gamma\begin{bmatrix} 0 & \alpha & 0 \\ 0 & -\alpha-r_3-r_2-\mu-\lambda & \epsilon F_{TI} \\ 0 & r_2 & -q-\epsilon F_{TI}-\mu-\lambda \end{bmatrix}$$

$$+r_3\begin{bmatrix} 0 & -\delta F_{LI}-\gamma-p-\mu-\lambda & 0 \\ 0 & \delta F_{TI} & \epsilon F_{TI} \\ 0 & p & -q-\epsilon F_{TI}-\mu-\lambda \end{bmatrix}-q\begin{bmatrix} 0 & -\delta F_{LI}-\gamma-p-\mu-\lambda & \alpha \\ 0 & \delta F_{LI} & -\alpha-r_3-r_2-\mu-\lambda \\ 0 & p & r_2 \end{bmatrix}=0$$

This also yields:

$$-\mu-\lambda\left[(-\delta F_{LI}-\gamma-p-\mu-\lambda)\left[(-\alpha-r_3-r_2-\mu-\lambda)(-q-\epsilon F_{TI}-\mu-\lambda)-r_2\epsilon F_{TI}\right]-\alpha\left[\delta F_{LI}(-q-\epsilon F_{TI}-\mu-\lambda)-p\epsilon F_{TI}\right]\right]=0$$

Utilizing the parameter values in Table 1 yields the following results:

$$\lambda = -0.08, -0.291, -0.2903, -1.2874$$

2.4 Basic Reproductive Number (R_0)

To find the reproductive number, only two stages are considered, i.e., the L and I stages. The equations are as follows:

$$\frac{\partial L}{\partial t}=\beta S F_{SL}\frac{I}{N}+C^{*}F_{TL}T\frac{I}{N}+\alpha I-\delta F_{LI}L-\gamma L-pL-\mu L \tag{12}$$

$$\frac{\partial I}{\partial t}=\delta F_{LI}L+\epsilon F_{TI}T-\alpha I-r_3 I-r_2 I-\mu I \tag{13}$$

Eq. (12) at equilibrium yields:

$$0=\beta F_{SL}S\frac{I}{N}+C^{*}F_{TL}T\frac{I}{N}+\alpha I-\delta F_{LI}L-\gamma L-pL-\mu L$$

This is equal to:

$$\beta F_{SL}S\frac{I}{N}=L\left(\delta F_{LI}+\gamma+p+\mu\right)-C^{*}F_{TL}T\frac{I}{N}-\alpha I \tag{14}$$

Eq. (13) at equilibrium yields:

$$0=\delta F_{LI}L+\epsilon F_{TI}T-\alpha I-r_3 I-r_2 I-\mu I$$

This is equal to:

$$\delta F_{LI}L=I\left(\alpha+r_3+r_2+\mu\right)-\epsilon F_{TI}T$$

To find the reproductive number, the following is equated:

$$\mathbf{F}(t)=\begin{bmatrix}\dfrac{\partial\left(\beta S F_{SL}\frac{I}{N}\right)}{\partial L} & \dfrac{\partial\left(\beta S F_{SL}\frac{I}{N}\right)}{\partial I}\\ \dfrac{\partial\left(\delta F_{LI}L\right)}{\partial L} & \dfrac{\partial\left(\delta F_{LI}L\right)}{\partial I}\end{bmatrix}=\begin{bmatrix}0 & \beta F_{SL}\frac{1}{N}\\ \delta F_{LI} & 0\end{bmatrix} \tag{15}$$

$$\mathbf{V}=\begin{bmatrix}\dfrac{\partial\left[L\left(\delta F_{LI}+\gamma+p+\mu\right)-C^{*}F_{TL}T\frac{I}{N}-\alpha I\right]}{\partial L} & \dfrac{\partial\left[L\left(\delta F_{LI}+\gamma+p+\mu\right)-C^{*}F_{TL}T\frac{I}{N}-\alpha I\right]}{\partial I}\\ \dfrac{\partial\left[\left(\alpha+r_3+r_2+\mu\right)-\epsilon F_{TI}T\right]}{\partial L} & \dfrac{\partial\left[I\left(\alpha+r_3+r_2+\mu\right)-\epsilon F_{TIT}T\right]}{\partial I}\end{bmatrix}=\begin{bmatrix}\delta F_{LI}+\gamma+p+\mu & -C^{*}F_{TL}T\frac{1}{N}-\alpha\\ 0 & \alpha+r_3+r_2+\mu\end{bmatrix}$$

$$\mathbf{V}^{-1}=\frac{1}{\left(\delta F_{LI}+\gamma+p+\mu\right)\left(\alpha+r_3+r_2+\mu\right)}\begin{bmatrix}\alpha+r_3+r_2+\mu & C^{*}F_{TL}T\frac{1}{N}+\alpha\\ 0 & \delta F_{LI}+\gamma+p+\mu\end{bmatrix}$$

Assuming that there is no interaction at the beginning, the equation can be expressed as follows, according to Georges (Kamanga, 2020):

$$\mathbf{FV}^{-1}=\frac{1}{(\delta F_{LI}+\gamma+p+\mu)(\alpha+r_3+r_2+\mu)}\begin{bmatrix}\alpha+r_3+r_2+\mu & C^*F_{TL}T\frac{1}{N}+\alpha\\ 0 & \delta F_{LI}+\gamma+p+\mu\end{bmatrix}\begin{bmatrix}0 & \beta F_{SL}\frac{1}{N}\\ \delta F_{LI} & 0\end{bmatrix}$$

$$\mathbf{FV}^{-1}=\frac{1}{(\delta F_{LI}+\gamma+p+\mu)(\alpha+r_3+r_2+\mu)}\begin{bmatrix}\left(C^*F_{TL}T\frac{1}{N}+\alpha\right)\delta F_{LI} & (\alpha+r_3+r_2+\mu)\beta F_{SL}\frac{1}{N}\\ (\delta F_{LI}+\gamma+p+\mu)\delta F_{LI} & 0\end{bmatrix}$$

$$\mathbf{FV}^{-1}=\begin{bmatrix}\frac{\left(C^*F_{TL}T\frac{1}{N}+\alpha\right)\delta F_{LI}}{(\delta F_{LI}+\gamma+p+\mu)(\alpha+r_3+r_2+\mu)} & \frac{(\alpha+r_3+r_2+\mu)\beta F_{SL}\frac{1}{N}}{(\delta F_{LI}+\gamma+p+\mu)(\alpha+r_3+r_2+\mu)}\\ \frac{(\delta F_{LI}+\gamma+p+\mu)\delta F_{LI}}{(\delta F_{LI}+\gamma+p+\mu)(\alpha+r_3+r_2+\mu)} & 0\end{bmatrix}=\begin{bmatrix}A & B\\ C & D\end{bmatrix}$$

As delineated by Georges (Kamanga, 2020), R_O can be calculated as follows:

$$R_o=\frac{-B\pm\sqrt{B^2-4AC}}{2A}$$

R_O is the biggest eigenvalue of matrix FV^{-1}, calculated according to:

$$R_o=\frac{-\frac{(\alpha+r_3+r_2+\mu)\beta F_{SL}\frac{1}{N}}{(\delta F_{LI}+\gamma+p+\mu)(\alpha+r_3+r_2+\mu)}\pm\sqrt{\left[\frac{(\alpha+r_3+r_2+\mu)\beta F_{SL}\frac{1}{N}}{(\delta F_{LI}+\gamma+p+\mu)(\alpha+r_3+r_2+\mu)}\right]^2-4\frac{\left(C^*F_{TL}T\frac{1}{N}+\alpha\right)\delta F_{LI}}{(\delta F_{LI}+\gamma+p+\mu)(\alpha+r_3+r_2+\mu)}\frac{(\delta F_{LI}+\gamma+p+\mu)\delta F_{LI}}{(\delta F_{LI}+\gamma+p+\mu)(\alpha+r_3+r_2+\mu)}}}{2\frac{\left(C^*F_{TL}T\frac{1}{N}+\alpha\right)\delta F_{LI}}{(\delta F_{LI}+\gamma+p+\mu)(\alpha+r_3+r_2+\mu)}}$$

$$R_o=\frac{-\frac{(0.099+0.15+0.8+0.08)*21*1\frac{1}{200,000,000}}{(0.2*1+0.001+0.2+0.08)(0.099+0.15+0.8+0.08)}\pm\sqrt{\left[\frac{(0.099+0.15+0.8+0.08)21*1*\frac{1}{200,000,000}}{(0.2*1+0.001+p+0.08)(0.099+0.15+0.8+0.08)}\right]^2-4\frac{\left(0.7*1*7,500,000\frac{1}{200,000,000}+0.099\right)0.2*1*}{(0.2*1+0.001+0.01+0.08)(0.099+0.15+0.8+0.08)}\frac{(0.2*1+0.001+0.01+0.08)0.2*1}{(0.2*1+0.001+0.01+0.08)(0.099+0.15+0.8+0.08)}}}{2\frac{\left(0.7*1*7,500,000\frac{1}{200,000,000}+0.099\right)0.2*1}{(0.2*1+0.001+0.01+0.08)(0.099+0.15+0.8+0.08)}}$$

$$R_o=\frac{-0.0000002183\pm\sqrt{\left[\frac{0.0000002183}{0.325}\right]^2-4*\frac{0.1253}{0.3285}*\frac{0.0582}{0.3285}}}{2*\frac{0.1253}{0.3285}}$$

$$R_o=\frac{-0.0000002183\pm\sqrt{0-0.27033632}}{0.7629}$$

$$R_o=0.3544i$$

Tables 1 and 2 describe the parameters of the model.

Table 1. Rate description in the model

Parameter	Interpretation
$\mu(1\text{-}p)N$	Birthrate of Individuals to Susceptible Populations
μS	Death rate due to Susceptible Populations S
μL	Death rate due to Latent L
μI	Death rate due to Infectious I
μT	Death rate due to Treatment T
γL	Number of latent individual recover to S due to natural recovery
αI	Number of Infectious individual recover to L due to natural recovery

$\epsilon F_{TI}T$	Number of treated individual who become chronic
μPN	Number of vaccinated Individuals
$\beta F_{SL}S\frac{1}{N}$	Number of people infected at Latent stage
$\delta F_{LI}L$	Number of infected individual from Latent statge to Infectious
r_2I	Number of individual who when for Treatment
r_3I	Number of infectious individual who recover Natural without treatment
qT	Number of treated individual who move to Susceptible after treatment
pT	Number of Latent who detect the early and want to hospital for treatment
$C^*F_{TI}T\frac{1}{N}$	Number of treated Individual who return to Latent stage

Table 2. Description of parameters of the model

Parameter	Interpretation		
μ	Death rate	0.08	(Saito & Nagasaki, 2008)
N	Population of Nigeria	200,000,000	(Sudre et al., 1992)
P	Vaccinated Individual	0.2	(Saito & Nagasaki, 2008)
(1-P)	unvaccinated Individual	0.8	(Saito & Nagasaki, 2008)
F_{TI}	Chronic contact Frequency	1	Assume
F_{LI}	Contact frequency of Latent Infectious L to Infectious I	1	Assume
F_{SL}	Contact rate of Susceptible S to Latent Infectious L	1	(Saito & Nagasaki, 2008)
γ	Ratio of contact susceptible individual S to latent infectious L	0.001	(Saito & Nagasaki, 2008)
α	Ratio of infectious I to latent infectious L	0.099	(Saito & Nagasaki, 2008)
ϵ	Ratio of treatment T to infectious I	0.15	(Saito & Nagasaki, 2008)
β	Ratio of susceptible S to latent infectious L	21	(Saito & Nagasaki, 2008)
δ	Ratio of individual from Latent L to Infectious I	0.2	(Saito & Nagasaki, 2008)
r_2	Ratio of individual from Infectious I to Treatment T	0.8	(Saito & Nagasaki, 2008)
r_3	Ratio of infectious individual who recover Natural without treatment	0.15	(Saito & Nagasaki, 2008)
q	Ratio of treated individual who move to Susceptible after treatment	0.2	(Saito & Nagasaki, 2008)
p	Ratio of Latent who detect the early and want to hospital for treatment	0.01	(Saito & Nagasaki, 2008)
C^*	Ratio of treated Individual who return to Latent stage	0.7	(Saito & Nagasaki, 2008)

3. Simulation and Result

Figure 2 shows the pictorial flow of each compartment model. The red line shows how the number of S individuals is decreasing due to the virus. The line rapidly decreases from the second year until the fifth year. The blue line shows the rapid increase of L individuals due to the higher contact rate. The number of I individuals is very high to the extent that it almost meets S individuals. The green line shows the I individuals and how the disease spreads to the population. The last line, which is purple, shows T people, whose number is greater than that of all the remaining compartments. The subgraph (a) of Figure 3 shows the comparison between the S and L individuals which meet at equilibrium approximately 3.5 years later. This shows that the virus really has a large impact due to its higher reproductive number. The number of L individuals continues to grow till it reaches the population size. Therefore, a lot of people may contract the disease, known or unknown. The subgraph (b) of Figure 3 displays the comparison between the S and T individuals. The more S decreases, the more T follows. It also shows that the government shows clear concern for the disease, but the population is affecting disease control once more. The subgraph (a) of Figure 4 shows the comparison between the I and T individuals. The vaccine and treatment yield good results, with the vaccinated T population being higher than the I population, which is awesome. The subgraph (b) of Figure 4 also shows the difference between the L and T individuals. Totally, 143 T individuals are also higher than the L individuals.

The subgraph (a) of Figure 5 shows the number of deaths per compartment. It can be seen that the S has the

highest number of deaths, maybe due to the population in the compartment. The number of *S* decreases during 0-2 years, increases rapidly from around 2.2-4 years, which is the extremely high point of the *S*, and finally decreases to almost zero. The number of *I* individuals also decreases at some point in the green line. At some point, the deaths of the *S* and *I* individuals are almost equal, which shows that the disease is killing people and individuals also die naturally, with the deaths reaching 4*108. The *L* individuals are represented by the blue line. The number also decreases drastically, and the death rate in the treatment also decreases rapidly, indicating that the intervention is effective. The subgraph (b) of Figure 5 shows how people are recovering from the disease. The treatment rate of recovery is very high compared to other compartments, followed by *S* individuals who recover within the period of 1.5 to 5.2 years before becoming stable after 5 years. The numbers of *I* and *L* individuals are also decreasing due to their willingness to receive the treatment and the assumption that they are leaving the compartment for medication. The subgraph (a) of Figure 6 shows the number of *I* individuals recovered to *S* without treatment. This shows that many *I* individuals have no symptoms and recover without awareness, but the virus has a higher value of risk in the fourth year. The yellow line represents the increase in *S*, while the purple line represents the decrease in *L*. Both compartments become stable after six years. The subgraph (b) of Figure 6 shows both the movement of how *I* people get cured without treatment and the fact that the number is higher than that of those moving to an *I* compartment. The negative value shows the release of individuals from their compartment, and the positive value shows their absorption in the compartment.

Figure 7 illustrates the number of patients discharged from the hospital due to their chronic condition or lack of response to medication. Therefore, the patients need to return home and enter the *I* compartment. As displayed in the figure, the blue line, which is *T*, decreases after the fourth year and increases after the second year of endemic. However, the red line, which is *I*, rapidly increases from zero year to the fourth, decreases after the fourth year till the sixth year, and continues to increase afterwards. This shows that the disease is still circulating among the masses and that the chronic disease has not been eradicated. The subgraph (a) of Figure 8 shows how the *I* compartments are losing individuals to the *T* ones. The numbers are equal in terms of the axis, and the negative value of *I* shows the number of people moving to *T* compartments for effective treatment. The disease is at equilibrium at five-and-a-half years. The subgraph (b) of Figure 8 shows the number of individuals vaccinated. The *T* has the highest vaccinated population, which is almost 7 million people, followed by the *I* population of more than 4 million, the *L* population of almost 30 million, and finally the *S* individuals. As shown in the figure, the number of *S* individuals is negative and converges to zero, which means people are moving from one compartment to another. The subgraph (a) and (b) of Figure 9 display the death rate for each compartment when the death rate parameter increases to 4.9. It can be seen that even if the death rate increases, the population dies in each compartment becomes stable in less than a year.

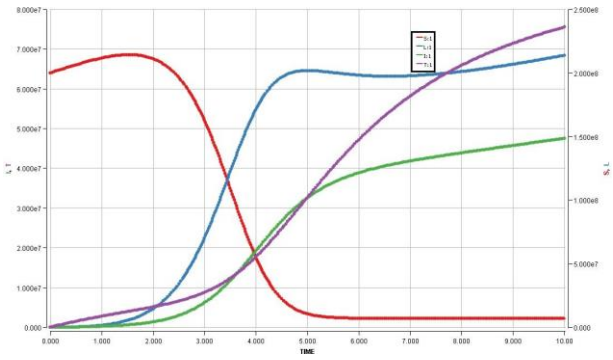

Figure 2. TB simulation results

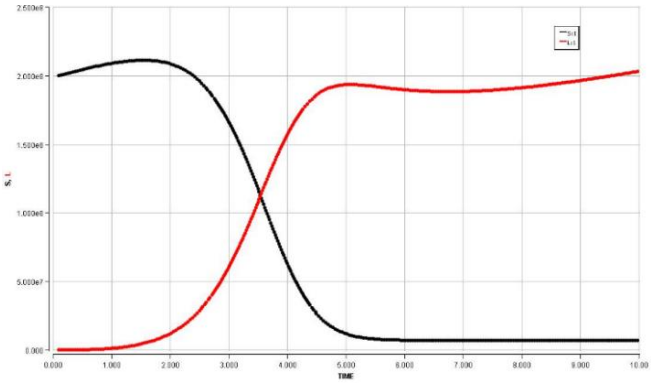

(a) Comparison between *S* and *L*

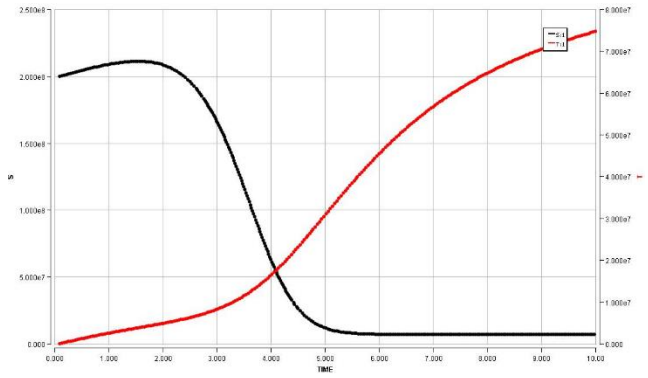

(b) Comparison between *S* and *T*

Figure 3. Comparative analysis between *S*, *L* and *T*

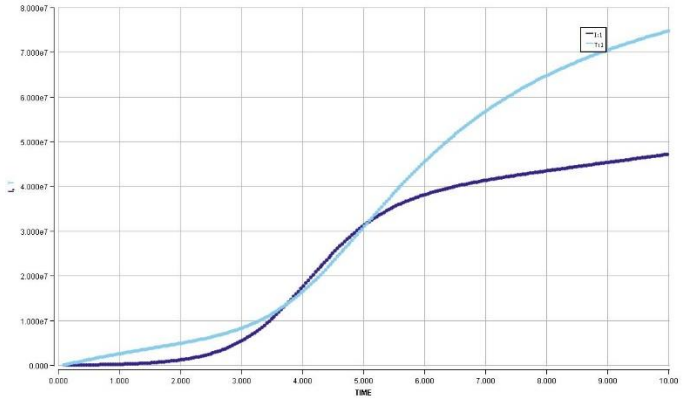

(a) Comparison between *T* and *I*

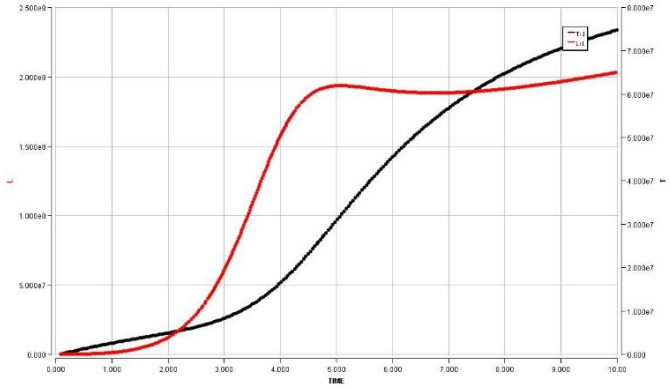

(b) Comparison between *T* and *L*

Figure 4. Comparative analysis between *T*, *I* and *L*

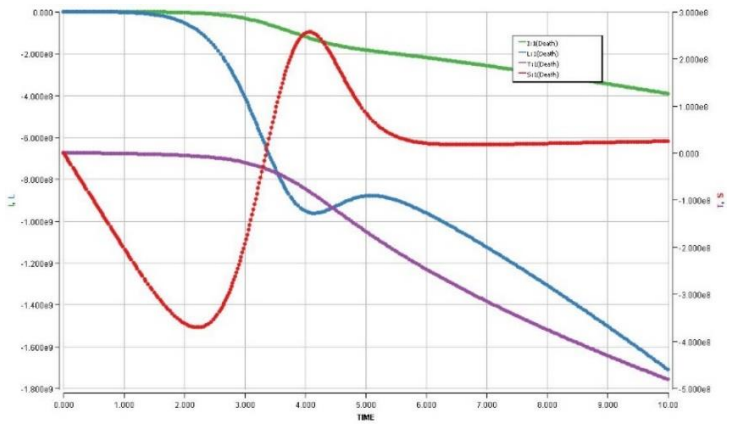

(a) Number of deaths per compartment

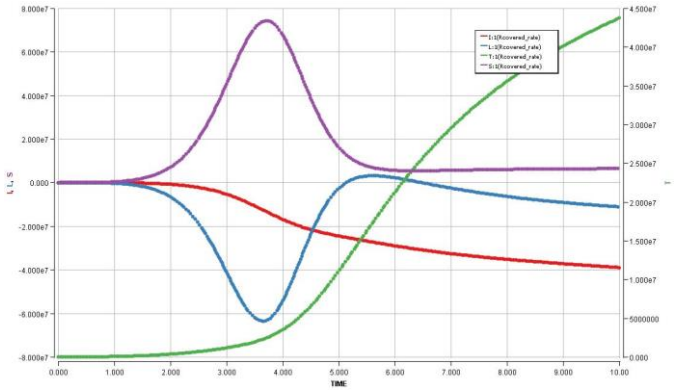

(b) Recovery rate per the compartment

Figure 5. Sensitivity analysis of death and recovery rate

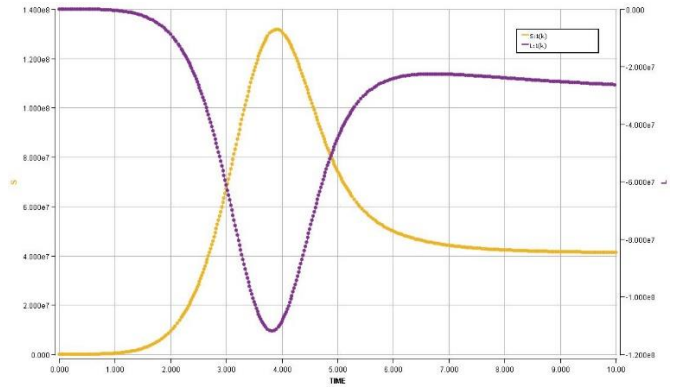

(a) Recovery from L without Treatment

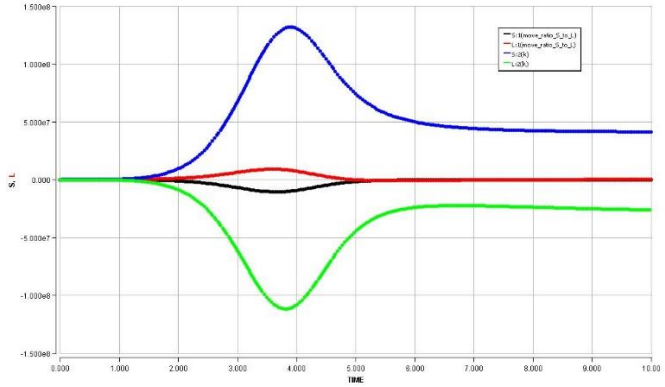

(b) Sensitivity analysis of *S* and *L* without treatment

Figure 6. Sensitivity analysis of non-treated individuals

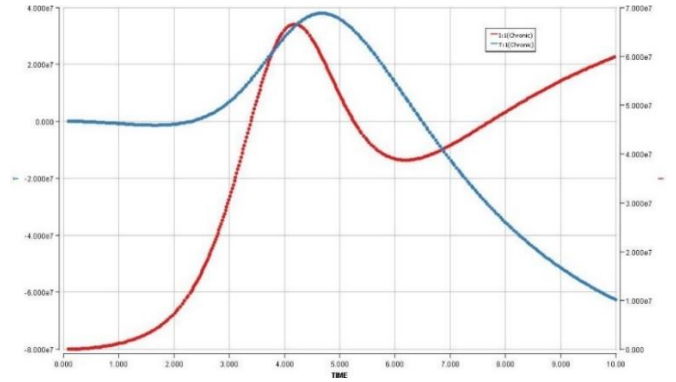

Figure 7. Chronic individuals

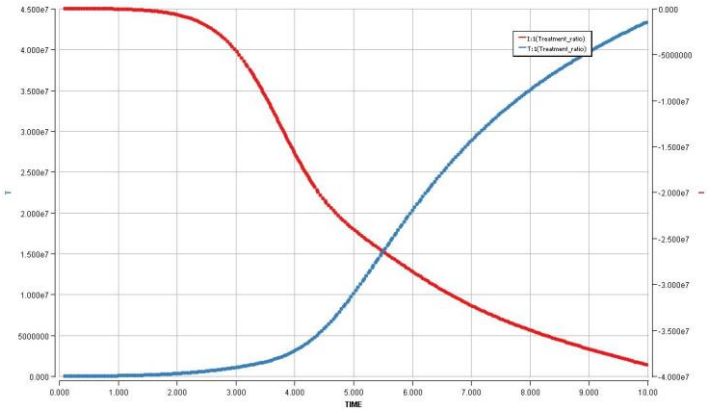

(a) T individuals

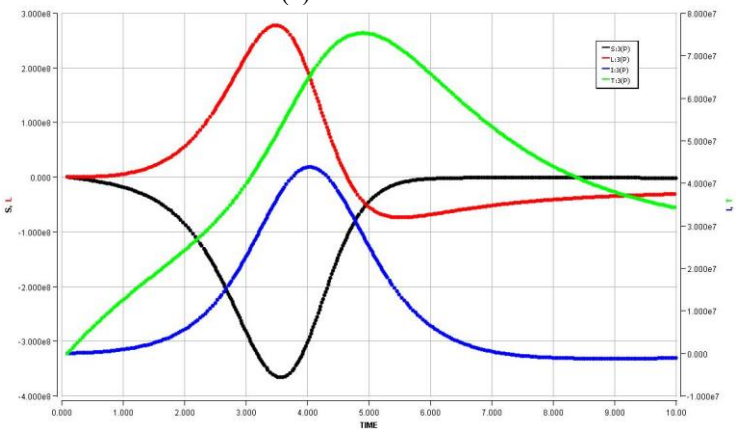

(b) Vaccinated individuals

Figure 8. Sensitivity analysis of T and vaccinated individuals

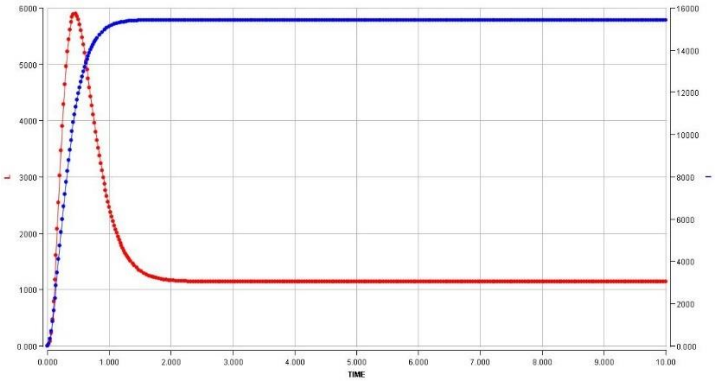

(a) Sensitivity analysis of μ on L and I

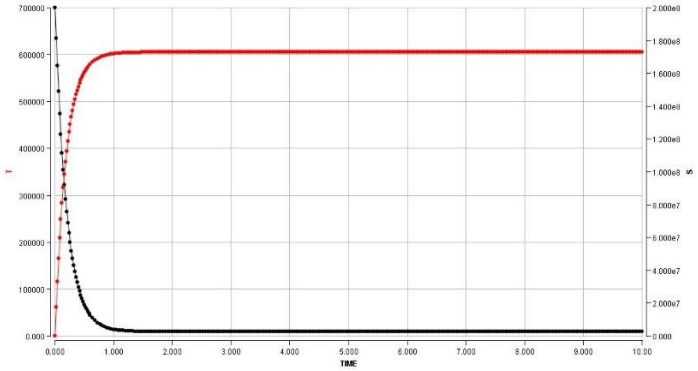

(b) Sensitivity analysis of μ on T and S citizens

Figure 9. Sensitivity analysis of μ

4. Conclusions

In this study, a mathematical model is developed for TB transmission by examining scenarios both in the presence and absence of treatment interventions. It can be found that the treated population is greater than the untreated population. Vaccinated and unvaccinated individuals are also compared. It can be found that vaccinated individuals are much higher than individuals in other compartments. Calculations reveal that the disease-free equilibrium and the basic reproductive number are less than one, indicating that the disease is under control. Or, it is unstable, indicating that the disease is not under control. In conclusion, the presented simulation shows that vaccination is able to prevent the disease from spreading.

Author Contributions

All the author contributes equally.

Ethical Approval

This study adheres to strict ethical guidelines, ensuring the rights and privacy of participants. Informed consent was obtained from all participants, and personal information was protected throughout the study. The methodology and procedures of this research have been approved by the appropriate ethics committee. Participants were informed of their rights, including the right to withdraw from the study at any time. All collected data is used solely for the purpose of this research and is stored and processed in a secure and confidential manner.

Data Availability

The data used to support the research findings are available from the corresponding author upon request.

Acknowledgements

This work is supported by Helpman Development Institute under a private institutional grant.

Conflicts of Interest

The authors declare no conflict of interest.

References

Atangana, A. & Doungmo Goufo, E. F. (2014). Computational analysis of the model describing HIV infection of CD4+ T cells. *Biomed Res. Int., 2014*. https://doi.org/10.1155/2014/618404.

Castillo-Chavez, C. & Song, B. (2004). Dynamical models of tuberculosis and their applications. *Math. Biosci. Eng., 1*(2), 361-404. https://doi.org/10.3934/mbe.2004.1.361.

Goufo, E. F. D., Maritz, R., & Pene, M. K. (2017). A mathematical and ecological analysis of the effects of petroleum oil droplets breaking up and spreading in aquatic environments. *Int. J. Environ. Pollut., 61*(1), 64-71. https://doi.org/10.1504/IJEP.2017.082699.

Goufo, E. F. D., Pene, M. K., & Mugisha, S. (2016). Stability analysis of epidemic models of Ebola hemorrhagic fever with non-linear transmission. *J. Nonlinear Sci. Appl., 9*(6), 4191-4205.

Huo, H. F. & Zou, M. X. (2016). Modelling effects of treatment at home on tuberculosis transmission dynamics. *Appl. Math. Model., 40*(21-22), 9474-9484. https://doi.org/10.1016/j.apm.2016.06.033.

Kamanga, G. (2020). Mathematical model of dynamics and control of police bribery in Rwanda. In *African Institute of Mathematical Sciences Cameroon*.

Kasereka, S., Kasoro, N., & Chokki, A. P. (2014). A hybrid model for modeling the spread of epidemics: Theory and simulation. In 2014 4th International Symposium ISKO-Maghreb: Concepts, Tools and Knowledge Management. (ISKO-Maghreb), Algiers, Algeria, 1-7. https://doi.org/10.1109/ISKO-Maghreb.2014.7033457.

Kasereka, S., Le Strat, Y., & Léon, L. (2018). Estimation of infection force of hepatitis C virusamong drug users in France. *Recent Adv. Nonlinear Dyn. Synch., 109*, 319-344. https://doi.org/10.1007/978-3-319-58996-1_15.

Leon, L., Kasereka, S., Barin, F., et al. (2017). Age-and time-dependent prevalence and incidence of hepatitis C virus infection in drug users in France, 2004–2011: Model-based estimation from two national cross-sectional serosurveys. *Epidemiol. Infect., 145*(5), 895-907. https://doi.org/10.1017/S0950268816003107.

Nainggolan, J., Supian, S., Supriatna, A. K., & Anggriani, N. (2013). Mathematical model of tuberculosis transmission with recurrent infection and vaccination. *J. Phys. Conf. Ser., 423*(1), 012059.

https://doi.org/10.1088/1742-6596/423/1/012059.
Ndondo, A. M., Munganga, J. M. W., Mwambakana, J. N., Saad-Roy, C. M., Van den Driessche, P., & Walo, R. O. (2016). Analysis of a model of gambiense sleeping sickness in humans and cattle. *J. Biol. Dyn., 10*(1), 347-365. https://doi.org/10.1080/17513758.2016.1146783.
Saito, Y. & Nagasaki, H. (2008). The melanin-concentrating hormone system and its physiological functions. *Orphan G Protein-Coupled Receptors and Novel Neuropeptides*, 159-179. https://doi.org/10.1007/400_2007_052.
Statistics, V. A. (2004). *National Bureau of Statistics*.
Sudre, P., Ten Dam, G., & Kochi, A. (1992). Tuberculosis: A global overview of the situation today. *Bull. World Health Organ., 70*(2), 149-159.
Sulayman, F. & Abdullah, F. A. (2022). Dynamical behaviour of a modified tuberculosis model with impact of public health education and hospital treatment. *Axioms, 11*(12), 723. https://doi.org/10.3390/axioms11120723.
Tchepmo Djomegni, P. M., Govinder, K. S., & Doungmo Goufo, E. F. (2018). Movement, competition and pattern formation in a two prey–one predator food chain model. *Comput. Appl. Math., 37*, 2445-2459. https://doi.org/10.1007/s40314-017-0459-4.
Ullah, S., Khan, M. A., Farooq, M., & Gul, T. (2019). Modeling and analysis of tuberculosis (TB) in Khyber Pakhtunkhwa, Pakistan. *Math. Comput. Simul., 165*, 181-199. https://doi.org/10.1016/j.matcom.2019.03.019.
World Health Organization. (2019). Global tuberculosis report. WHO: Geneva, Switzerland.

Nomenclature

μ	Death rate
N	Population of Nigeria
P	Vaccinated Individual
(1-P)	unvaccinated Individual
F_{TI}	Chronic contact Frequency
F_{LI}	Contact frequency of Latent Infectious L to Infectious I
F_{SL}	Contact rate of Susceptible S to Latent Infectious L
γ	Ratio of contact susceptible individual S to latent infectious L
α	Ratio of infectious I to latent infectious L
ϵ	Ratio of treatment T to infectious I
β	Ratio of susceptible S to latent infectious L
δ	Ratio of individual from Latent L to Infectious I
r_2	Ratio of individual from Infectious I to Treatment T
r_3	Ratio of infectious individual who recover Natural without treatment
q	Ratio of treated individual who move to Susceptible after treatment
p	Ratio of Latent who detect the early and want to hospital for treatment
C^*	Ratio of treated Individual who return to Latent stage